Prediction of End-point RH Refining Furnace Based on Improved Whale Optimization Algorithm and Stochastic Configuration Network

C. Shi, P. Sun, T. Zhou, B. Wang, Y. Wang, L. Zhang

A model for predicting the end-point temperature and end-point carbon content of RH refining steel based on an improved whale optimization algorithm and a stochastic configuration network (LWOA-SCN) is proposed to solve the existing problem of inaccurate detection of the steel composition in the ladle during the steelmaking process. The algorithm has an implicit layer structure that can be generated adaptively based on the training effect and has the ability of strong generalization performance, simple structure, fast convergence, high accuracy, and jumping out of local optimum. Firstly, the LWOA-SCN algorithm is used to construct the prediction model. Secondly, the model was tested against RBF, GA-BP, and PSO-SVM models, and the results showed that the LWOA-SCN model had the highest predicted effect. Finally, the LWOA-SCN model was tested in industrial production applications, and the results showed that the hit rate is 90.6%, 95.6%; 93.7%, 94.3% for refining end-point temperature and end-point carbon content error within ±5°C, ±10°C; and ±0.005%, ±0.01%, respectively. which can well meet the practical needs of a steel mill. The model provides theoretical guidance and production guidance for studying the control of refining end-point temperature and end-point carbon content.

KEYWORDS: RH REFINING, STOCHASTIC CONFIGURATION NETWORK, LEVY FLIGHT ALGORITHM, IMPROVED WHALE OPTIMIZATION ALGORITHM, END-POINT TEMPERATURE AND END-POINT CARBON CONTENT PREDICTION MODEL

INTRODUCTION

With the increasingly fierce competition of steel mills, the quality of products is more and more valued by enterprises, and the fluctuation of end-point carbon content and end-point temperature in steelmaking has a great influence on the adjustment of process parameters and the performance of final products. The high superheat of the continuous casting molten steel temperature and the deviation of the molten steel temperature drop from the target value can have a direct impact on the product quality. The results show that the equiaxed crystallinity of molten steel decreases with the increase of superheat, and the shrinkage, porosity, segregation, and crack are closely related to the superheat, thus reducing the competitiveness of the product. According to the production process, the average RH refining process time in a steel mill is about 40 min. reducing a temperature measurement, smelting efficiency can be increased by

Chunyang Shi
School of Electrical and Automation Engineering, Liaoning Institute of Science and Technology, China - Liaoning Provincial Engineering Research Center of Robotic Drive and Control, China.

Peng Sun, Baoshuai Wang, Yikun Wang, Lei Zhang
School of Electrical and Automation Engineering, Liaoning Institute of Science and Technology, China

Tian Zhou
Benxi Beiying Steel (Group) Co. Benxi, China.

scy9090@126.com.

10%[1]. Therefore, it is necessary to reduce the number of manual temperature measurements in the refining process to reduce the smelting time, reduce energy consumption, and control production costs.

More and more attention has been paid to the role of refining, and RH vacuum refining technology has become a widely used technology in various mills. It mainly has the following metallurgical functions: dehydrogenation, decarburization, deoxidation, desulfurization, precise control of molten steel composition and temperature, inclusion control, and removal. The varieties suitable for smelting are greatly increased, and it has become indispensable refining equipment for smelting high-grade pipelines, ultra-low carbon steel, silicon steel, and other high value-added steels. The precision of end-point temperature and end-point carbon content control of refining determines whether the steel quality meets the standard. The traditional process mainly adopts the combination of mechanism analysis and empirical control. It mainly analyzes the change of molten steel temperature through the influence of ladle thermal state and other factors on molten steel temperature based on heat transfer theory[2-5]. However, the main drawback of this method is that the temperature and carbon content change of molten steel in the ladle is affected by many factors in the actual production process, and they are in a strong coupling and strong nonlinear relationship, so it is difficult to consider comprehensively, which leads to the phenomenon that the traditional mechanism analysis method will have complex prediction process, slow control speed and unguaranteed prediction accuracy[6-10].

To achieve the precise requirement of end-point temperature and end-point carbon content control, intelligent control methods tried by domestic and foreign researchers are attempted to control the end-point temperature and end-point carbon content[11-13]. With previous research on the subject, the study of refining models based on intelligent algorithms has become a hot issue in automated steelmaking. Many scholars have carried out in-depth research on the prediction and control of the refining end-point temperature and end-point carbon content by using methods such as neural networks, fuzzy logic systems, and so on, and achieved certain research results. Whereas there are still some shortcomings in the prediction accuracy and end-point hit rate, because the influence factors are not comprehensive enough, the algorithm is easy to fall into a local minimum, poor training ability of small samples, and low computational efficiency[14-17]. To address the aforementioned issues, this work develops prediction model employing the LWOA-SCN algorithm for controlling end-point temperature and end-point carbon content in the RH refining production process for an actual 210 t ladle in a steel mill. By comparing this model with RBF, GA-BP, and PSO-SVM prediction models, a study of the model accuracy is carried out to verify the superiority of the proposed model, which provides a theoretical basis for the problem of optimal control of end-point temperature and end-point carbon content in the actual production of a steel mill.

The subject belongs to the latest application in the field of metallurgical intelligent control, combining metallurgical technology with predictive technology in a favorable way. It is another new milestone in the development of metallurgical technology, breaking the deficiencies of the end-point temperature and end-point carbon content control in the traditional process and transforming what might otherwise be produced as a substandard product into a qualified product by pre-adjusting the process parameters online. It reduces the scrap rate and reduces production costs at the same time.

INDUSTRIAL TRIALS

RH refining process is a method of vacuum circulation degassing. After forming a closed container inside the vacuum tank, turn on the vacuum pump, and the vacuum is formed above the molten steel. Under atmospheric pressure, the molten steel is pressed into the vacuum tank, so that the molten steel enters from the riser and flows out from the downcomer to complete the degassing and decarburization of the molten steel.

The experiment process is carried out by the actual production RH refining process in a steel mill. The RH refining process is shown in Fig 1. After the ladle reaches the RH refining process position, the ladle is started to enter the station for temperature measurement, and then blow argon with a large flow rate. While the ladle is vacuumed, a certain amount of alloy is added. According to the process requirements. The vacuum is stopped, and the temperature is measured after 15 min. Then, the vacuum is continued for the ladle, and the alloy is added to reduce the argon blowing rate until it is stopped. Finally, the ladle temperature is measured once more, the end-point temperature of the RH refining process.

During the whole refining process, the temperature of

molten steel is measured by a thermocouple at the early, middle, and late stages of the experiment. In order to improve the accuracy of the temperature of molten steel, it is measured by the average value of multi-point temperature measurement (5-point temperature measurement is used during the experiment) and the insertion depth is 210 mm (the distance is longer than the height of slag surface above the molten steel, so as it can yield accurate measurement of the steel temperature). Finally, the measured temperature is displayed on the monitor. The RH refining process structure and temperature measurement point position are shown in Fig 2.

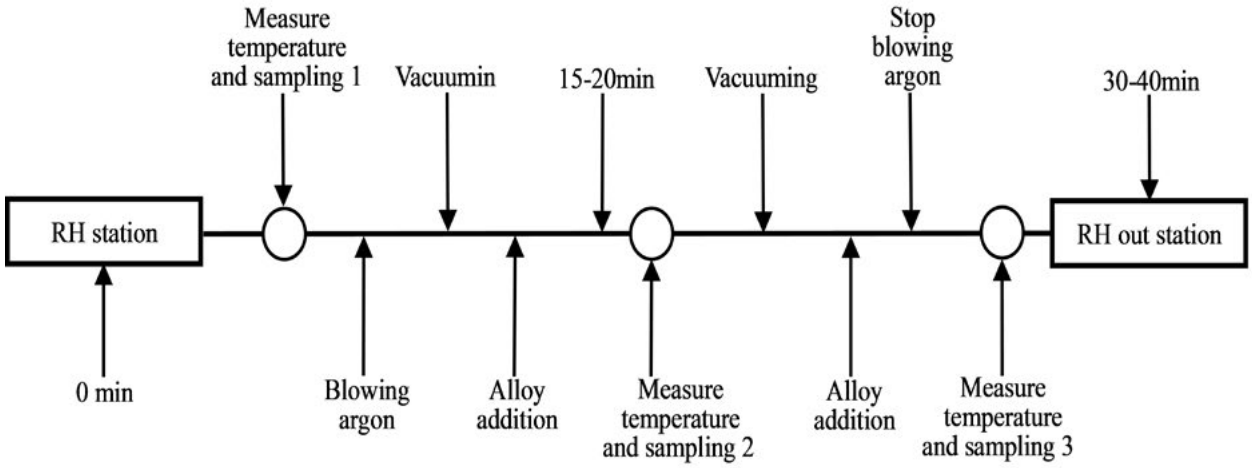

Fig.1 - Structural diagram of RH refining process experiment.

During the industrial trials online data of 210 t ladle refining were collected. The different liquidus temperatures of different steel grades were taken into account in the data collection process, which resulted in the different refining end-point temperature and end-point carbon content required by the process. Therefore, the same steel grade was used as the research object (the most representative low carbon steel SPCC was used as the research object in this experiment), a total of 2000 furnace times.

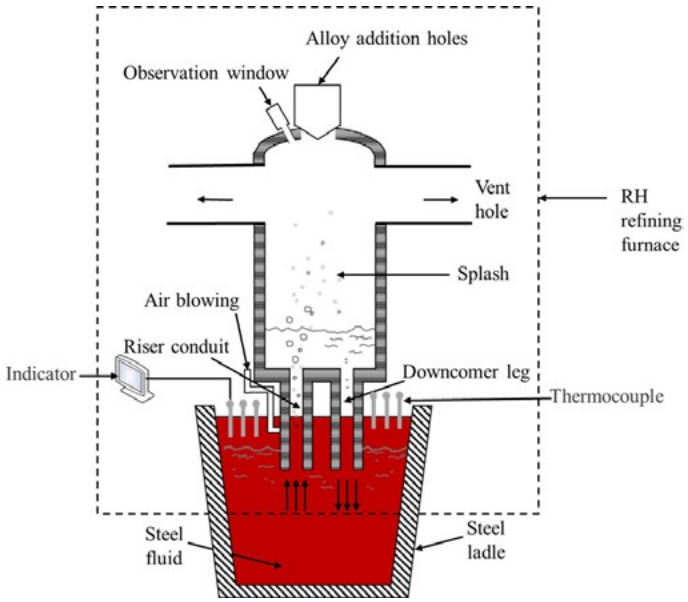

Fig.2 - Structural diagram of RH refining process experiment.

END-POINT PREDICTION MODEL OF RH REFINING BASED ON LWOA-SCN

Sample data processing

In this paper, the error data and noise data are removed according to the Laida criterion to obtain the online detection data of 2000 groups of steel. of which 75% (1500 groups) are taken as the training sets; 25% (500 groups) are taken as the test sets, and the correlation analysis is carried out using SPSS to obtain the correlation coefficients of each factor, and several factors with small correlation coefficients are excluded. The corresponding data table is shown in Table 1. Finally, 7 parameters, including the start temperature of refining, the tonnage of molten steel, refining time, alloy addition amount, the amount of slag added, the thickness of slag, and the ladle age, are obtained as the input factors of the model. The correlation between the factors is shown in table 1.

Due to the large and complex nature of the raw data, large forecasting errors caused by order of magnitude differences in the different dimensions of the data are eliminated. Therefore, it is necessary to normalize the input and output of the established model by mapping the input and output data to the [0,1] interval data normalization using the following equation.

$$x_i' = \frac{x_i - \min(x_i)}{\max(x_i) - min(x_i)}, \quad i = 1,2,3,\dots,m \tag{1}$$

where:

min (x_i), the minimum value of the model input or output raw data;

max (x_i), the maximum value of the model input or output raw data;

(x_i), the raw data of the model input or output.

Tab.1 - Data correlation analysis table.

Dependent variable	Variable	Correlation coefficient
Output parameters of the model	The start temperature of refining	0.556
	Refining time	-0.120
	Alloy addition amount	-0.224
	The amount of slag added	-0.264
	The tonnage of molten steel	0.113
	The thickness of slag	0.165
	Ladle age	0.029

Improved whale optimization algorithm

Compared with other optimization algorithms, the WOA algorithm has a faster operation speed, simple adjustment parameters, and a certain ability to jump out of the local optimum. However, since the algorithm itself only uses a random system for exploration, and the excessive dependence on random limits the search speed of the WOA algorithm, the convergence speed and convergence accuracy of the WOA algorithm are further accelerated. In addition, due to the limitation of coefficient vector B, the WOA algorithm will lose the ability to jump out of the local optimum when the number of iterations reaches half of the maximum set number of iterations. Therefore, the WOA algorithm has a certain risk of falling into the local optimum, resulting in inaccurate prediction results of the algorithm. To solve the above defects of the WOA algorithm, Levy flight is used to improve the WOA algorithm. The improved algorithm has a faster convergence speed and higher convergence accuracy and has a better ability to jump out of the local optimum. Levy flight is a search based on Levy distribution, which is a random way of small-range search and large-range jump. Established using the following mathematical model for the predatory strategy of humpback whales:

$$X(t+1) = X^*(t) - BD_1 \quad (2)$$

where:
t, the current number of iterations;
B and M, coefficient vectors.

$$B = 2aLevy(\lambda) - a \quad (3)$$

$$M = 2r_2 \quad (4)$$

The WOA algorithm is used to solve the optimization problem for SCN. The whale optimization strategy is shown in Equation (5). The WOA algorithm is iterated iteratively to find the final solution.

$$X(t+1) = \begin{cases} \begin{cases} X^*(t) - lH, if a < 1 \\ X_{rand}(t) - lH, if a \geq 1 \end{cases}, if\ n < 0.5 \\ X^*(t) + \tau_p e^{\varepsilon \cdot m} \cdot \cos(2\pi m), if\ n \geq 0.5 \end{cases} \quad (5)$$

where:
l, constant; update the magnitude of the distance;
H, vector of coefficients;
X*(t), the position vector of the current optimal solution;
X(t), the current position vector of the humpback whales;
Xrand(t), the random position vector of the whale population;
τ_p, the distance between the whale population and the prey;
a, the variable that decreases from 2 to 0;
ε, describes the shape of the spiral motion;
m, a random vector in the interval [–1, 1];
n, probability variable.

In the established model process, the industrial trial data are quickly used and normalized. Then the input variables are determined, and 7 input variables are optimized by the LWOA algorithm. The search range of variables is [–1, 1], the number of populations is 30, and the number of iterations is 500. The first iteration randomly generates 30 groups of initial solutions, calculates the fitness of each group of solutions, and saves the group of solutions with the smallest fitness as the current optimal solution to complete this iteration. When entering the next iteration, according to the whale optimization strategy, the positions of 30 solutions are updated, and a group of solutions with the smallest fitness is compared with the current optimal solution to save the group of solutions with smaller fitness. After 500 iterations, the group of solutions with the smallest fitness is the global optimal solution, and then the optimization value of the input variable is obtained by inverse normalization processing, and the optimization process is completed.

SCN algorithm

Compared with the traditional machine learning model, the hidden layer structure of SCN can be generated adaptively based on the training effect, and it can start from a small network, then, new hidden nodes are added gradually with random parameters until the training precision of the network meets the termination condition, and the network has strong generalization performance. The basic structure diagram of the SCN is shown in Fig 3.

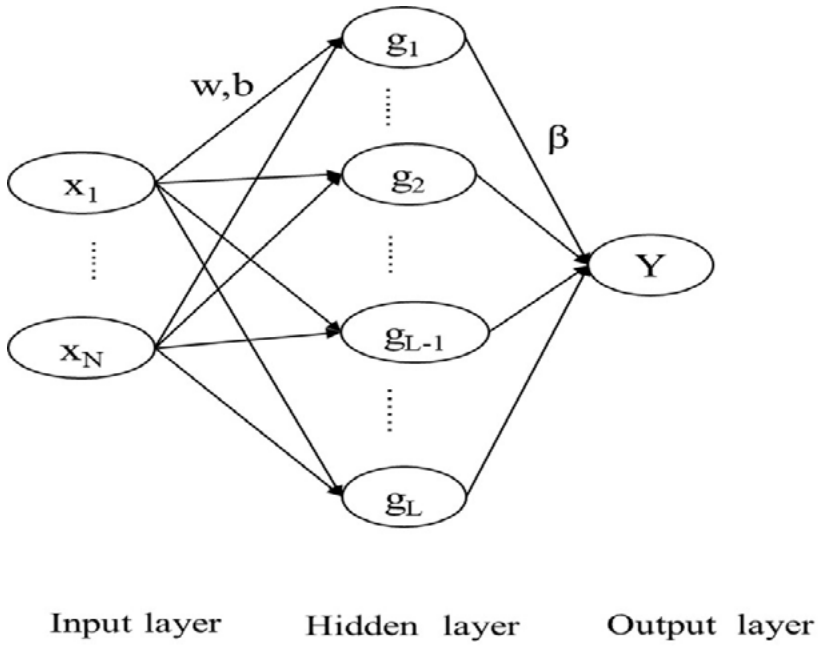

Fig.3 - The basic structure diagram of the SCN.

The specific steps for SCN are as follows:

Step 1: Given the objective function f: $R^M \rightarrow R^K$, after the L-1 addition of the node, the output of the current network is:

$$f_{L-1}(x) = \sum_{l=1}^{L-1} \beta_l g_l(w_l{}^T x + b_l) \tag{6}$$

Residuals for the current network:

$$e_{L-1} = f - f_{L-1} = [e_{L-1,1}, \cdots e_{L-1,m}] \tag{7}$$

If the residual $\|e_{L-1}\|$ does not meet the expected tolerance range, a new hidden node is added (a set of w_L, β_L, and b_L) such that the approximation function is:

$$f_L(x) = f_{L-1}(x) + \beta_L g_L(w_L{}^T x + b_L) \tag{8}$$

Step 2: when adding a new hidden node, the input weight vector w_L and deviation vector β_L are generated randomly. Where a pair of randomly generated w_L, β_L satisfy the following inequalities:

$$\sum_{q=1}^{m} < \langle e_{L-1,q}, g_L{}^* \rangle^2 \geq \|g_L{}^*\|^2 \delta_L \tag{9}$$

where:

$$g_L{}^* = g_L(w_L{}^T x + b_L) \tag{10}$$

$$\delta_L = (1 - r - u_L)\|e_{L-1}\|^2 \tag{11}$$

$$\mu_L = (1 - r)/(L + 1) \qquad 0 < r < 1 \tag{12}$$

Step 3: Calculate the output weights.

$$\beta_{L,q} = \frac{\langle e_{L-1,q}, g_L \rangle}{\|g_L\|^2}, q = 1,2,\dots m \tag{13}$$

Step 4: Calculate whether the error e_L is smaller than the pre-given error criterion: if it is satisfied, the SCN model training is completed, otherwise, continue to add intermediate layer nodes according to step 2 until the error criterion is satisfied.

If the specified error tolerance is not reached, the model will generate new hidden layer nodes under the constraint and satisfy the trend of decreasing deviation as the number of nodes increases, finally achieving $\lim_{L-\infty} \|f - f_L\| = 0$.

$$f_L = \sum_{l=1}^{L} \beta_L \sigma_L \tag{14}$$

The model outputs the weights according to the updated model as follows:

$$[\beta_l^*, \beta_2^*, \beta_3^*, \cdots \beta_L^*] = arg\min_{\beta} \left\| f - \sum_{l=1}^{L} \beta_l \sigma_l \right\| \tag{15}$$

where:

$$\beta_l^* = [\beta_{l,1}^*, \beta_{l,2}^* \cdots, \beta_{l,m}^*] \tag{16}$$

When the number of training samples is small, the L2 norm penalty term is introduced into the objective function of the model to avoid over-fitting of the SCN and to improve the generalization performance of the network.
The objective function of SCN is improved as follows:

$$[\beta_l^*, \beta_2^*, \beta_3^*, \cdots \beta_L^*] = arg\min_{\beta} \left\| f - \sum_{l=1}^{L} \beta_l \sigma_l \right\| + C\|\beta\| \tag{17}$$

where:
C, the penalty weight coefficient of the model.
The least squares output weight is defined as:

$$\beta^* = (GG^T + \lambda I)^{-1} GT \tag{18}$$

$$G = \sigma(w^T x + b) \tag{19}$$

$$\beta^* = [\beta_l^*, \beta_2^*, \beta_3^*, \cdots \beta_L^*]^T \tag{20}$$

The penalty parameter C of SCN is optimized by the LWOA algorithm. The relational flow chart of the LWOA optimized SCN is obtained as shown in Fig 4. Firstly, the actual production data are extracted and normalized, then the parameters of the SCN are optimized by the LWOA, and then the regression model is trained and tested with the optimal solution. Finally, the prediction model of end-point carbon content and end-point temperature is obtained by inverse normalization of the regression production data.

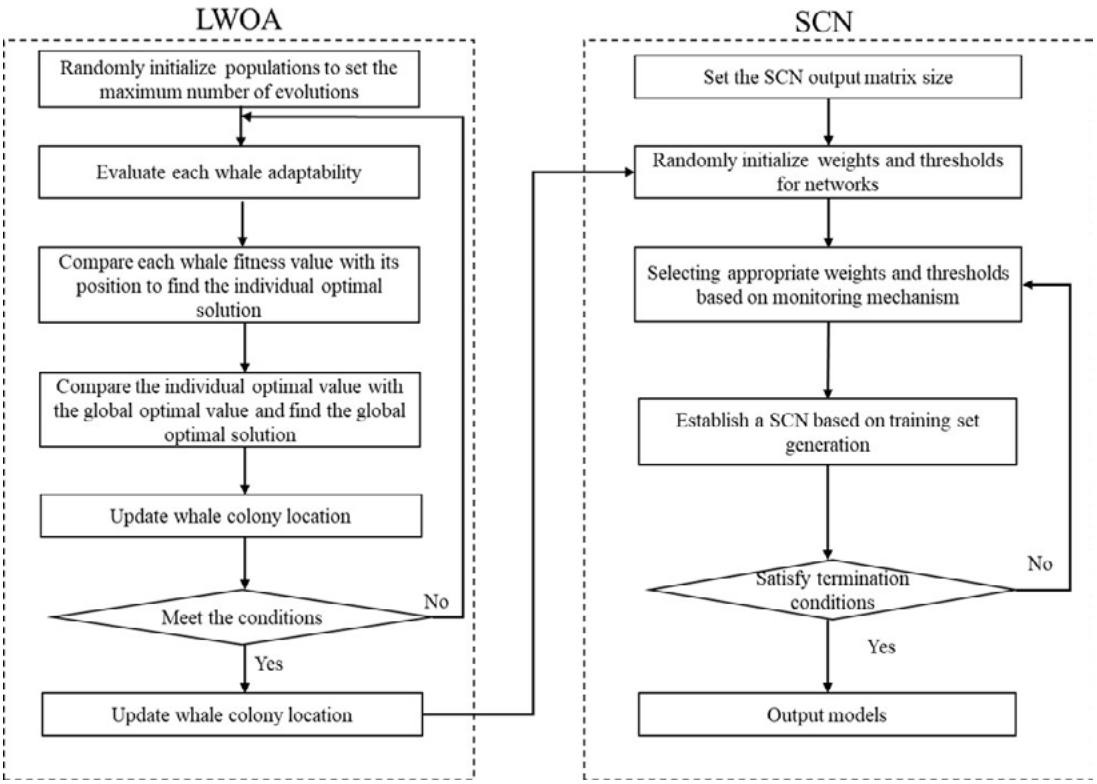

Fig.4 - The process of LWOA optimized SCN.

Through the above steps, the forecasting effect of the end-point carbon content and end-point temperature prediction model of the LWOA-SCN is finally obtained and compared with the actual value, as shown in Fig 5 and Fig 6.

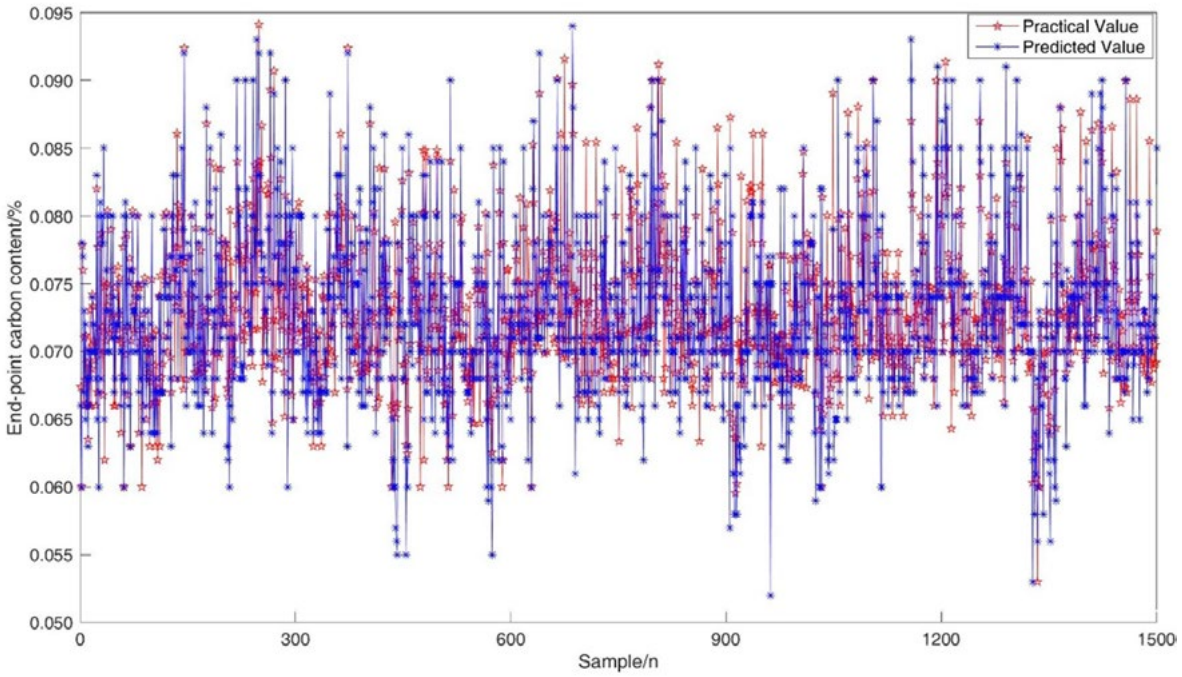

Fig.5 - The predicted effect of end-point carbon content.

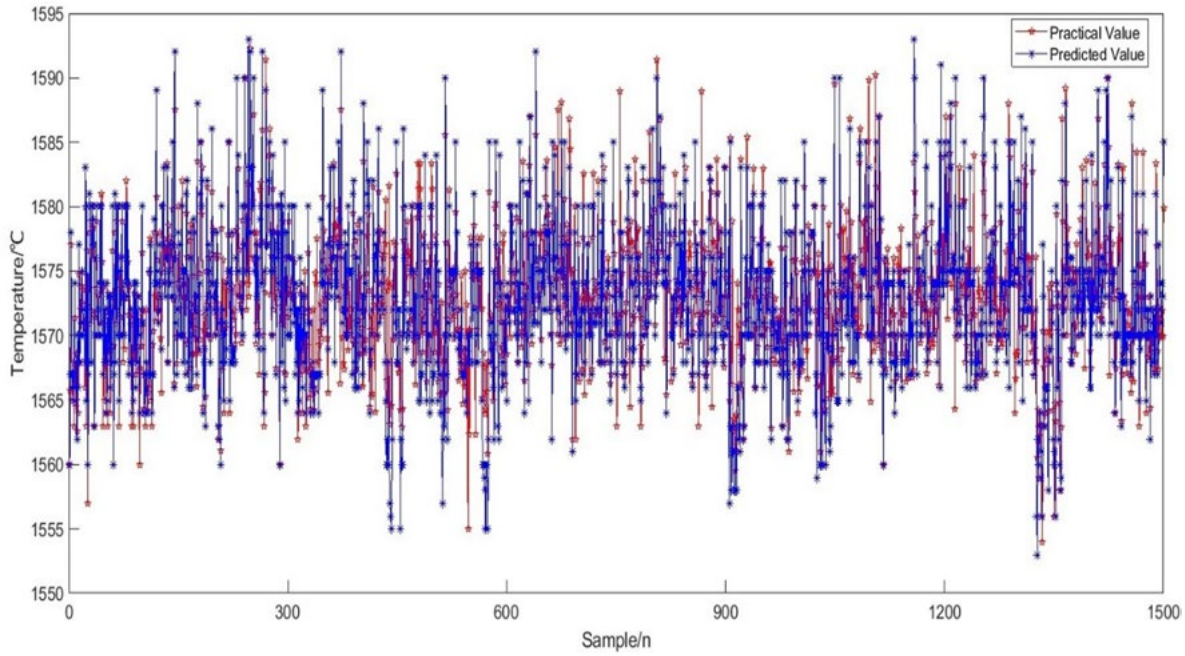

Fig.6 - The predicted effect of end-point temperature.

COMPARISON OF THE MODEL AND RESULT ANALYSIS

To examine the prediction effectiveness of the LWOA-SCN algorithm relative to the typical algorithm, four algorithms (RBF, GA-BP, PSO-SVM, and LWOA-SCN) are used to build the corresponding models for comparison. SSR/SST and SSE/SST are used to judge the fitting effect of the models, where the closer the SSR/SST value is to 1, the closer the oscillation between the model prediction and the practical value is to the same degree; the smaller the SSE/SST value is, the better the fit between the model prediction and the practical value is. The MAE, RMSE, and Relative error are used to evaluate the prediction accuracy of the model, and the HR (hit rate) is used to examine the degree to which the model met the standard. The predicted values of the four algorithms are compared with the actual production data, and the results are shown in Fig 7 and Fig 8.

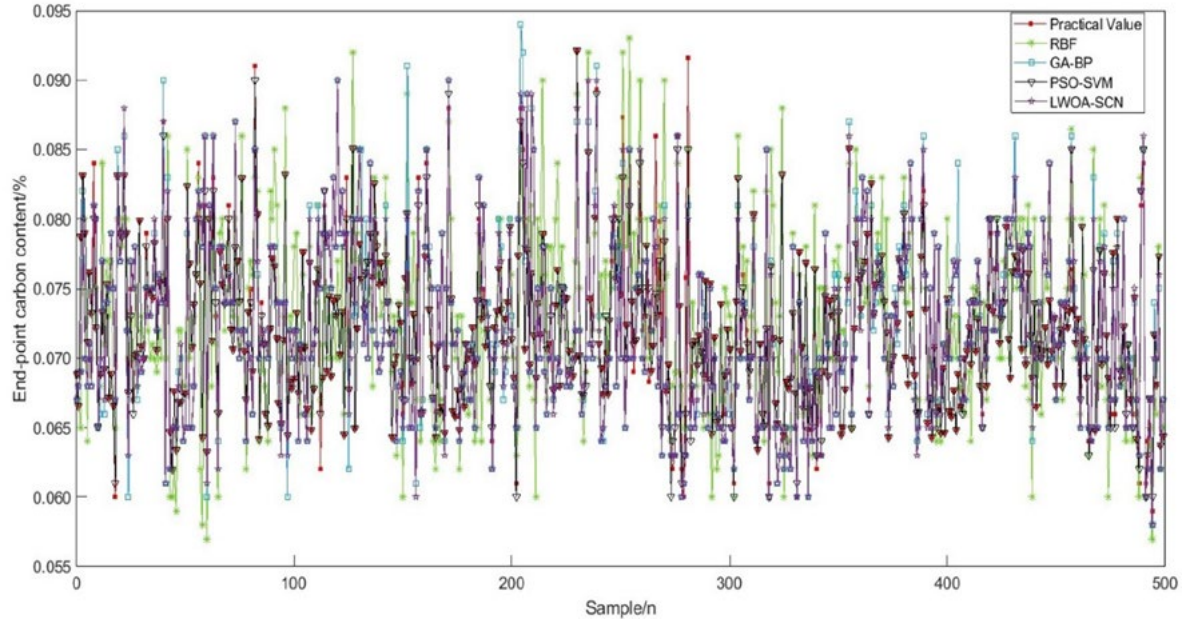

Fig.7 - Comparison of end-point carbon content results.

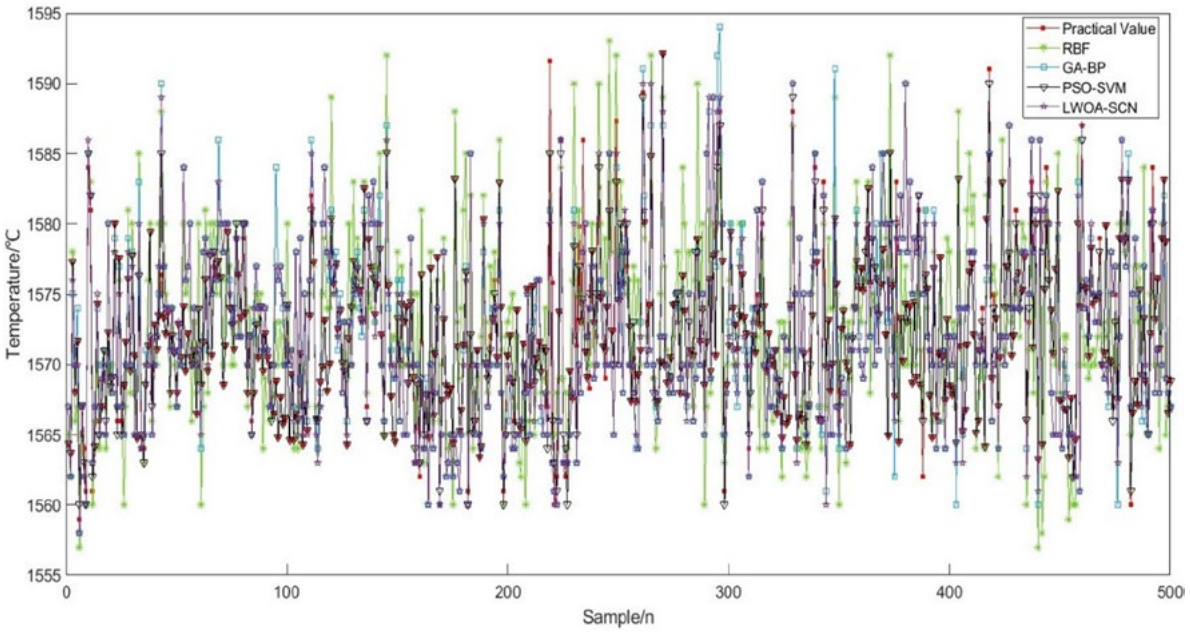

Fig.8 - Comparison of end-point temperature results.

As can be seen from Fig 7 and Fig 8, the deviations from the actual production data of the four models are in the order of small to large: LWOA-SCN, PSO-SVM, GA-BP, and RBF. According to the evaluation indexes of the four models in Table 2, it can be seen that among the end-point carbon content prediction models, the RMSE and MAE of the LWOA-SCN model are smaller than the other three algorithms, and the SSR/ SST is closer to 1, and the oscillation between predicted and true values is closer; the SSE/SST value is the lowest, and the model obtained the best fit. Finally, the LWOA-SCN model has the smallest RMSE and MAE compared to the other three algorithms, and SSR/SST is closer to 1, SSE/SST is also the lowest, and the best fit obtained by the model.

Tab.2 - Comparison of the regression effects of the four models.

Model	Evaluating indicator	RBF	GA-BP	PSO-SVM	LWOA-SCN
End-point carbon content model	RMSE	0.0041	0.0037	0.0032	0.0020
	MAE	0.0038	0.0032	0.0028	0.0021
	SSE/SST	0.3895	0.2456	0.1189	0.0134
	SSR/SST	0.6105	0.7544	0.8811	0.9866
End-point temperature model	RMSE	9.8972	7.0937	5.8272	4.3786
	MAE	8.7663	6.3496	5.7218	4.7628
	SSE/SST	0.2265	0.1321	0.0757	0.0237
	SSR/SST	0.7735	0.8679	0.9243	0.9763

To investigate the prediction accuracy of these models, this paper uses relative error as the error indicator to analyze the models. The smaller the value of relative error indicates the higher the prediction accuracy of the models. The calculation formula is Equation (21), and the relative error of LWOA-SCN, PSO-SVM, GA-BP, and RBF models are shown in Fig 9 and Fig 10.

$$\delta = \frac{\left|\hat{y}_i - y_i\right|}{y_i} \tag{21}$$

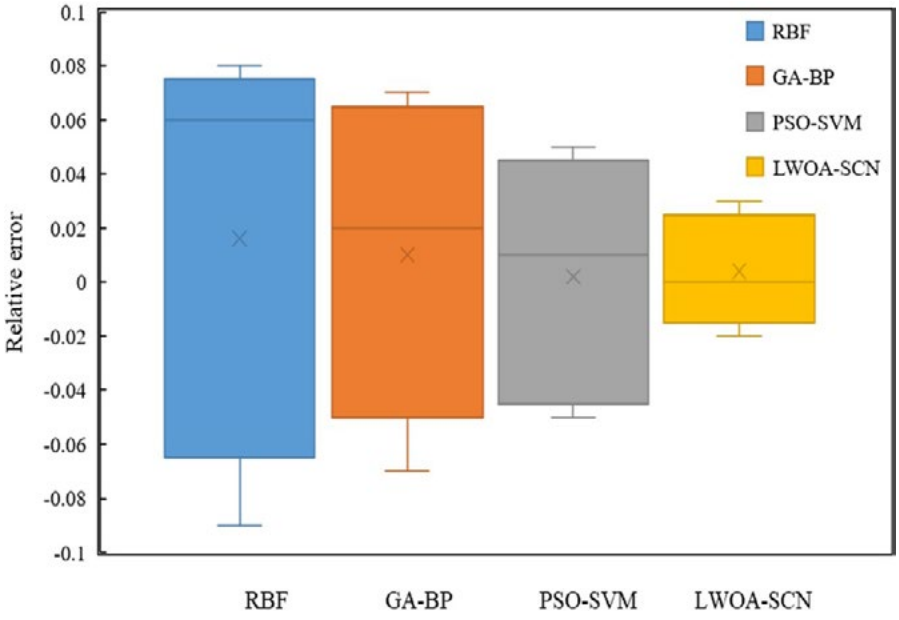

Fig.9 - Comparisons of relative error of end-point carbon content models.

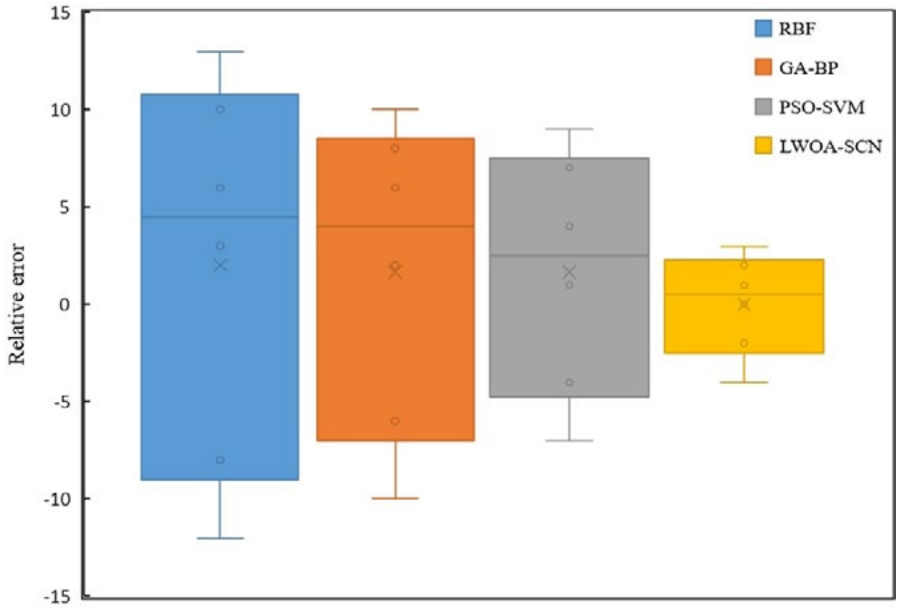

Fig.10 - Comparison of relative error of end-point temperature models.

From Fig 9 and Fig 10, it can be seen that the relative error of LWOA-SCN is the smallest among the four algorithms for both the end-point carbon content model and the end-point temperature model. The LWOA-SCN prediction model outperforms the other models.

To investigate the degree of compliance of the model, the HR (hit rate) performance index is used for the analysis. In the analysis of the prediction model, the prediction results are considered as hits when the end-point carbon content and end-point temperature satisfy Equation (22), and

the corresponding hit rate calculation formula is shown in Equation (23). From Table 3, the LWOA-SCN model has the highest hit rate under the same conditions, thus indicating that the prediction accuracy of this method is better than other algorithms.

$$C_S * (100\% - k) < C_y < C_S * (100\% + k) \tag{22}$$

where:
C_s, the measured results of the model;
C_y, results of model forecast;
k, Hit accuracy.

$$HR = \frac{\left(\left|y_i - \hat{y}_i\right| \leq n_e\right)}{n} * 100\% \tag{23}$$

In summary, according to the actual production data of a steel mill, through the comparison of RMSE, MAE, SSE/SST, SSR/SST, Relative error, and HR, the prediction performance evaluation index of the LWOA-SCN prediction model is the best, and the end-point hit rate is higher, indicating that the LWOA-SCN algorithm has higher approximation accuracy. It is verified that the LWOA-SCN prediction model has higher prediction performance. The model can be used to guide the actual production.

Tab.3 - The hit rate of the models.

Hit rate		Various model			
		RBF	GA-BP	PSO-SVM	LWOA-SCN
End-point carbon content model	Δw([C])≤0.005%	65%	78%	88%	93%
	Δw([C])≤0.01%	69%	82%	91%	94%
End-point temperature model	Δt≤5°C	75%	80%	88%	90%
	Δt≤10°C	79%	84%	90%	95%

APPLICATION AND VALIDATION

To verify the practical application of the established LWOA-SCN prediction model, the model is applied to a steel mill for actual production tests. Fig 11, and Fig 12 show the predicted data for 300 furnace times with the model applied. The hit rate is 90.6%, 95.6%; 93.7%, 94.3% for refining end-point temperature and end-point carbon content error within ±5°C, ±10°C; and ±0.005%, ±0.01%, respectively.

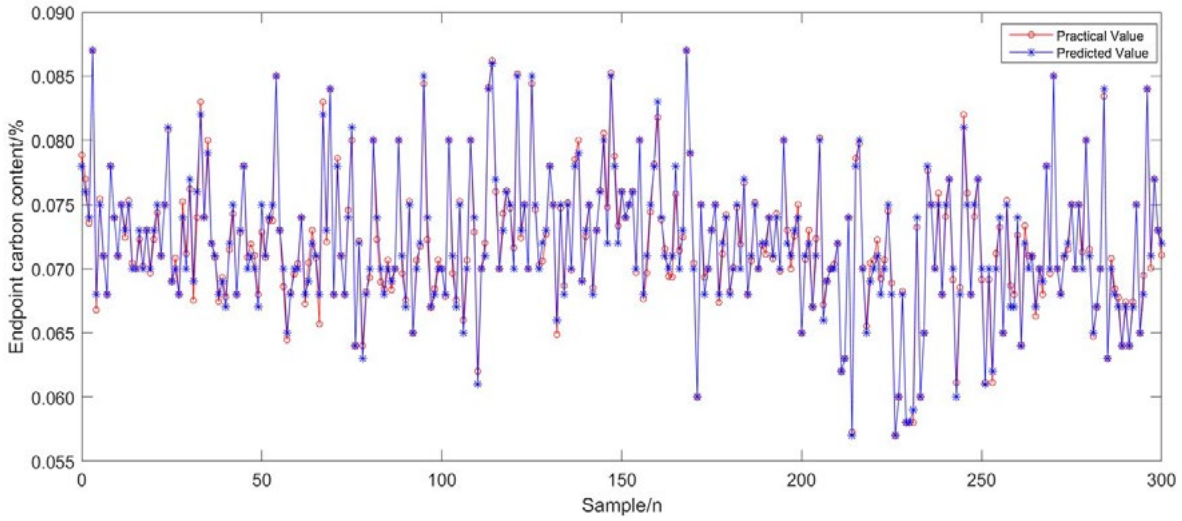

Fig.11 - Comparison of predicted and practical values of end-point carbon content model in the application.

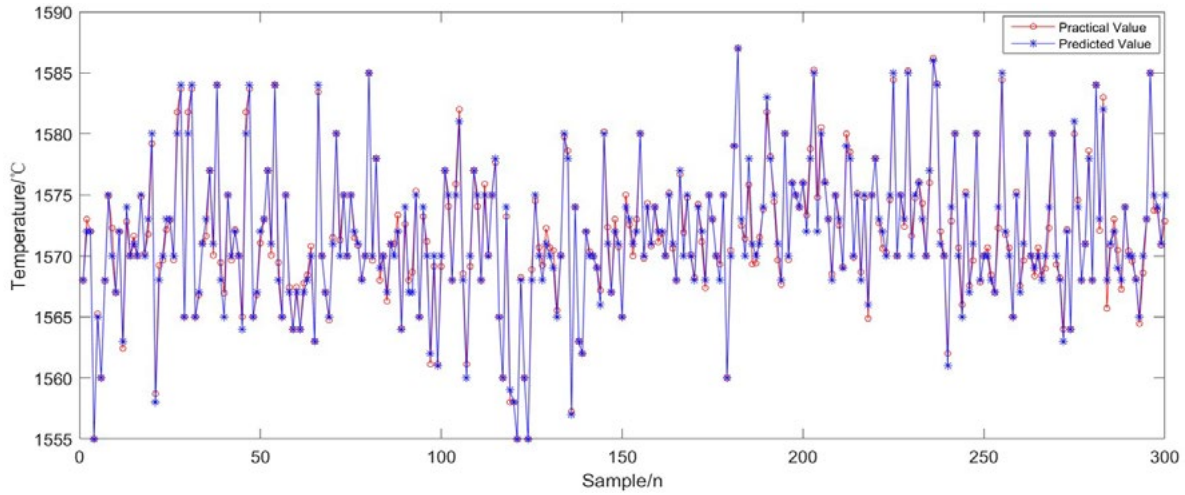

Fig.12 - Comparison of predicted and practical values of the end-point temperature model in the application.

CONCLUSION

In this paper, we propose a prediction model for RH refining end-point temperature and end-point carbon content based on LWOA-SCN, which has the advantages of fast convergence and high accuracy. The main conclusions are as follows:

(1) The prediction model of end-point temperature and end-point carbon content of RH refining based on the LWOA-SCN algorithm overcomes the shortcomings of traditional modeling's slow convergence speed and low convergence precision and improves the model's generalization ability and accuracy.

(2) The predicted data for 300 furnace times with the model applied. The hit rate is 90.6%, 95.6%; 93.7%, 94.3% for refining end-point temperature and carbon content error within ±5°C, ±10°C; and ±0.005%, ±0.01%, respectively.

(3) It is validated by the comparison of four forecasting models. The results show that the LWOA-SCN model has the smallest MAE, RMSE, and Relative error, thus verifying that the LWOA-SCN prediction model has good generalization ability. The model provides theoretical and production guidance for studying the control of refining end-point temperature and carbon content.

ACKNOWLEDGMENTS

This research was supported by the basic scientific research fund projects of the Educational Department of Liaoning Province in 2023(JYTMS20231800); the Liaoning Institute of Science and Technology doctoral research initiation fund project in 2023(2307B04) and the natural science fund program projects of the Department of Science & Technology of Liaoning Province in 2022(2022-BS-297).

REFERENCES

[1] Z.C. Xin, J.S. Zhang, J. Zheng, Y. Jin, Q. Liu. A hybrid modeling method based on expert control and deep neural network for temperature prediction of molten steel in LF[J]. ISIJ international 62(3) (2022)532-541.
[2] Y.D. Zhang. Research of temperature prediction model in the process of RH refining process[D]. Taiyuan university of science and technology (2016).
[3] D.f. He, F. He, A.J. Xu, N.Y. Tian. Online molten steel temperature control in steelmaking and continuous casting process[J]. Journal of Engineering Science: S1(2014)200-206.
[4] N. Kikuchi. Development and prospects of refining techniques in steelmaking process. ISIJ International 60.12(2020)2731-2744.
[5] Y.N. Wang, Y.P. Bao, H. Cui, B. Chen, C.X. Ji, Final temperature prediction model of molten steel in RH-TOP refining process for IF steel production[J]. Journal of Iron and Steel Research, International 19(3) (2012)1-5.
[6] C. Gao, M.G. Shen, X.P. Liu, L.D Wang, M. Chen. End-point Prediction of BOF Steelmaking Based on KNNWTSVR and LWOA[J]. Transactions of the Indian Institute of Metals, 2019, 72: 257-270.
[7] J.P. Yang, J.S. Zhang, W.D. Guo. S. Gao, Q. Liu, End-point temperature preset of molten steel in the final refining unit based on an integration of deep neural network and multi-process operation simulation[J]. ISIJ International 61(7) (2021)2100-2110.
[8] Z.C. Xin, J.S. Zhang, J.G. Zhang, Z. Jin, J. Yu, Q. Liu, Predicting Temperature of Molten Steel in LF-Refining Process Using IF–ZCA–DNN Model[J]. Metallurgical and Materials Transactions B, 54(3) (2023)1181-1194.
[9] H.X. Tian, Z.Z. Mao, An ensemble ELM based on modified AdaBoost. RT algorithm for predicting the temperature of molten steel in ladle furnace[J]. IEEE Transactions on Automation Science and Engineering 7(1) (2009)73-80.
[10] K. Feng, A.J. Xu, D.F. He, H.B. Wang, Prediction of RH refining process molten steel endpoint temperature based on integrated case reasoning method[J]. Journal of Engineering Science 40(S1) (2018)161-167.
[11] K. Feng, D.F. He, A.J. Xu, H.B. Wang, End Temperature Prediction of Molten Steel in LF Based on CBR-BBN[J]. Steel Research International 87(1) (2015)79–86.
[12] W. Lv, Z.Z. Mao, P. Yuan. Ladle Furnace Steel Temperature Prediction Model Based on Partial Linear Regularization Networks with Sparse Representation[J]. Steel Research International 83(3) (2013)288-296.
[13] F. He, A.J. Xu, H.B. Wang, D.F. He, N.Y. Tian, End Temperature Prediction of Molten Steel in LF Based on CBR[J]. Steel Research International 83(11) (2012)1079-1086.
[14] F. Yuan, A.J. Xu, M.Q. Gu, Development of an improved CBR model for predicting steel temperature in ladle furnace refining[J]. International Journal of Minerals, Metallurgy and Materials 28(2021)1321-1331.
[15] L.Z. Yang, B. Li, Y.F. Guo, S. Wang, B.T. Xue, S.Y. Hu, Influence Factor Analysis and Prediction Model of End-Point Carbon Content Based on Artificial Neural Network in Electric Arc Furnace Steelmaking Process[J]. Coatings 12(10) (2022)1508.
[16] L.M. Liu, P. Li, M.X. Chu, C. Gao. End-point prediction of 260 tons basic oxygen furnace (BOF) steelmaking based on WNPSVR and WOA[J]. Journal of Intelligent & Fuzzy Systems 41(2) (2021)2923-2937.
[17] C.Y. Shi, X.X. Yin, R. Chen, R.X. Zhong, P. Sun, B.S. Wang, S.Y. Guo, S.D. Li, Z.C. Ma, Prediction of end-point LF refining furnace based on wavelet transform based weighted optimized twin support vector machine algorithm[J]. Metallurgical Research & Technology 120(1) (2023)1.

TORNA ALL'INDICE >